High Refractive Index Inverse Vulcanized Polymers for Organic Photonic Crystals

Christian Tavella [1,2], Paola Lova [1,*] , Martina Marsotto [2], Giorgio Luciano [2], Maddalena Patrini [3], Paola Stagnaro [2,*] and Davide Comoretto [1]

[1] Dipartimento di Chimica e Chimica Industriale, Università degli Studi di Genova, Via Dodecaneso, 31, 16132 Genova, Italy; christian.tavella@scitec.cnr.it (C.T.); davide.comoretto@unige.it (D.C.)

[2] Istituto di Scienze e Tecnologie Chimiche "Giulio Natta", Consiglio Nazionale delle Ricerche, Via De Marini, 6, 16149 Genova, Italy; martina.marsotto@gmail.com (M.M.); giorgio.luciano@scitec.cnr.it (G.L.)

[3] Dipartimento di Fisica, Università degli Studi di Pavia, Via Bassi, 6, 27100 Pavia, Italy; maddalena.patrini@unipv.it

* Correspondence: paola.lova@edu.unige.it (P.L.); paola.stagnaro@scitec.cnr.it (P.S.)

check for updates

Abstract: Photonic technologies are nowadays dominated by highly performing inorganic structures that are commonly fabricated via lithography or epitaxial growths. Unfortunately, the fabrication of these systems is costly, time consuming, and does not allow for the growth of large photonic structures. All-polymer photonic crystals could overcome this limitation thanks to easy solubility and melt processing. On the other hand, macromolecules often do not offer a dielectric contrast large enough to approach the performances of their inorganic counterparts. In this work, we demonstrate a new approach to achieve high dielectric contrast distributed Bragg reflectors with a photonic band gap that is tunable in a very broad spectral region. A highly transparent medium was developed through a blend of a commercial polymer with a high refractive index inverse vulcanized polymer that is rich in sulfur, where the large polarizability of the S–S bond provides refractive index values that are unconceivable with common non-conjugated polymers. This approach paves the way to the recycling of sulfur byproducts for new high added-value nano-structures.

Keywords: polymer photonic crystals; inverse vulcanization; distributed Bragg reflectors; refractive index

1. Introduction

In the last few decades, photonic crystals have become of increasing technological relevance due to their potential of serving in many applications including lasers, optical switchers, and sensors [1–3]. Thus far, such applications have been circumscribed to inorganic structures that offer large dielectric contrast and the possibility to obtain several geometries via lithographic and epitaxial methods [2]. Inorganic materials offer almost defect-free structures that are characterized by a large dielectric contrast and performing light confinement. On the other hand, these systems require complex, costly, and time-consuming fabrications methods that can hardly be applied on a very large area. To this end, polymers promise to reduce fabrication costs and simplify processes while allowing for the easy obtainment of square meter scale structures [4–6]. Actually, large area and industrial fabrications have already been reported for colloidal opals that are made of self-assembled microspheres [7] and for multilayered distributed Bragg reflectors (DBRs) [8–10]. The latter are being increasingly studied for light management applications [11–14] and sensing purposes. Unfortunately, polymers offer refractive index values (n) in the transparency region ranging from 1.35 for fluorinated compounds to about 1.7 for aromatic non-conjugated species [2]. The limited dielectric contrast that is available between

commercial polymers is thus making the engineering of the refractive index important to achieve capability and commercial applications that, so far, have been limited to inorganic systems [15,16].

Several approaches have been employed to engineer the refractive index in polymer systems. Low indexes can indeed be obtained by using low density amorphous per-fluorinated macromolecules, where the strong electronegativity of the fluorine atom reduces electronic polarizability [17–20], or by using porous systems, where the large void volume fraction reduces the refractive index of the polymer matrix accordingly to effective medium theories [15,21–23]. Unfortunately, the solution processing of such polymers is still an open issue. Concerning high refractive index polymers, materials with n values larger than 2 in the near ultraviolet spectral region have been used to fabricate lenses for lighting devices [21–23], but the extension of such values to the visible and near infrared spectral windows is challenging, especially if accompanied by high transparency. Indeed, large values in the ultraviolet region can be obtained thanks to a pre-resonant enhancement that quickly disappears when approaching the visible spectral region [24,25]. To overcome such limitations, researchers have focused on polymer doping with high index inorganic nanoparticles, such as metal oxides and diamonds [11,19,26–28]. In these cases, a large volume fraction of the nano-load increases the refractive index of the ensuing composite medium [19,29]. A different approach relies on the covalent addition of highly polarizable groups or atoms including conjugated moieties and sulfur or selenium in the polymer backbone [30]. In these terms, hyperbranched polysulfides are very promising, even though only few researchers have reported on the fabrication of photonic crystals from them [31–33]. It is indeed known that, due to the high polarizability of the S–S bond, elemental sulfur possesses a high molar refractive index and excellent transparency in the near infrared region of the spectrum. Recently, polymers with very high content of S–S bonds were proposed by Char and Pyun as very high refractive index polymer materials (n~1.8) with excellent transparency in the near-infrared spectral region [34]. These sulfur-based polymers appear particularly intriguing from the applicative point of view due to their stability, thermoplastic behavior, and self-healing characteristics [35,36]. Such systems can be obtained by means of an efficient and simple synthetic process called inverse vulcanization (IV) and take the name of inverse vulcanized polymers (IVPs) [36,37]. In the IV process, molten sulfur, also acting as a solvent, is typically bulk copolymerized via free radical copolymerization with comonomers that bear vinylic moieties, such as 1,3-diisopropenylbenzene [34,36,38], thus leading to random copolymers. The inverse vulcanization process is thus an original and efficient method to exploit elemental sulfur to obtain new polymers and materials with unique functional properties. Sulfur is one of the most abundant and inexpensive elements on Earth, as well as a major by-product of oil refinery processes, and it also has a role as a common reaction site within biological systems [39]. Research involving sulfur has spanned a broad spectrum of topics within the physical sciences [40], including research on improving energy efficiency, environmentally friendly uses for oil refinery waste products, the development of polymers with unique optical and mechanical properties, and materials that are produced for biological applications.

In this work, we demonstrate the use of new IVPs that were created via the copolymerization of elemental sulfur (S) with 2,5-diisopropenylthiophene (DIT) comonomer in the fabrication of all-polymer DBRs. Due to their relatively low glass transition temperature, the prepared random Ssulfur-DIT copolymers (S-*r*-DIT) were blended with poly(*N*-vinyl carbazole) (PVK, n = 1.67 at 600 nm), a widely used polymer in the fabrication of plastic DBRs [2,13,41,42], to improve their processability. The obtained blends were employed as high refractive index medium that was alternated to polyacrylic acid (PAA, n = 1.45 at 600 nm) as the low index medium in the fabrication process.

2. Materials and Methods

Synthesis of 2,5-di(prop-1-en-2-yl)-thiophene: Elemental sulfur in powder (S, Ph. Eur., BP), 2,5-dibromothiophene (95%), 4,4,5,5-tetramethyl-2-(prop-1-en-2-yl)-1,3,2-dioxaborolane (isopropenylboronic acid pinacol ester, 95%), Cs_2CO_3 (99%), $Pd(PPh_3)_4$ (99%), 1,4-dioxane ($\geq$ 99.5%), as well as other chemicals and solvents, were purchased from Sigma-Aldrich (Italy) and used as

received. As in a typical synthesis, 8.109 g of Cs_2CO_3 (24.89 mmol, 4 eq.), 0.108 g of $Pd(PPh_3)_4$ (9.03×10^{-2} mmol, 1.5 % mol), and 0.70 mL of 2,5-dibromothiophene (6.20 mmol, 1 eq.) were added under an Ar atmosphere in a two-necked flask that was equipped with a magnetic stirrer and a bubble condenser. In a separate flask, a mixture (30 mL) of 1,4-dioxane/H_2O (2:1) was prepared while bubbling with Ar for 30 min. The solvent mixture was then added to the reaction flask while mixing the liquid phase and the suspended solid catalyst for 40 min under magnetic stirring. Then, 3.5 mL (18.60 mmol, 3 eq) of isopropenylboronic acid pinacol ester were dropped into the reaction flask that was heated in an oil bath (T = 90 °C) and maintained under reflux for 24 h. A brown oil was obtained and purified on chromatographic column to isolate a yellow, low-melting crystalline solid (yield 89%).

Inverse Vulcanization: The IVPs were synthesized via the copolymerization of elemental sulfur with DIT as the comonomer at different S/DIT weight ratios. The IV reaction was carried out by means of an experimental set-up that exploited a Büchi glass oven that operated in controlled temperature conditions and under an Ar atmosphere. The proper amounts of S and DIT were placed in a Teflon vessel that was equipped with a lid and magnetic stirrer. The temperature was raised from 25 to 170 °C in 7 min, kept at 170 °C for 70 min while maintaining the magnetic stirring, and finally lowered to 25 °C in 20 min.

DBR Fabrication: The obtained IVPs were then purified by dissolution and filtration in toluene to remove possible immiscible impurities that could affect the photonic structure quality. The process allowed for the obtainment of IVP solutions with a concentration of 10 mg/mL in toluene. To enhance filmability and processability of the IVPs, PVK was further dissolved in the IVP solutions to reach a concentration of PVK of 10 mg/mL. After stirring, the IVP:PVK solutions were used to fabricate the DBRs by using PAA (35 mg/mL in 2-methyl-2-pentanol) as a low refractive index polymer. All the multilayers were fabricated by casting 21 alternated layers (realizing 10.5 periods) of the two mentioned orthogonal polymer solutions by spin-coating while using a constant rotation speed (160 round per second) and deposition volumes (75 μL).

Characterization Methods: Thermogravimetric analysis (TGA) was carried out with a Perkin Elmer 8000 analyzer (Perkin Elmer, Waltham, MA, USA) by heating the polymer specimens (ca. 15 mg) under N_2 from 25 up to 700 °C and then under O_2 up to 850 °C (gas flow 40 mL/min). Two or three measurements were done for each sample. Effective S/DIT ratios were determined by the carbonaceous residue (wt%) at 700 °C.

Differential scanning calorimetry (DSC) measurements on IVPs (ca. 15 mg) were performed with a Mettler DSC 821^e instrument (Mettler Toledo, Columbus, OH, USA) by heating at 20 °C/min from −50 up to 200°C under an N_2 atmosphere (flow 40 mL/min). The reported values of glass transition temperature (T_g) were the average of two or three replicas for each sample.

Spectroscopic ellipsometry measurements were performed by using a VASE instrument (J. A. Woollam Co, Lincoln, NE, USA) in the range 250–2500 nm at different incidence angles from 55° to 75° on films that were deposited on both quartz and Silicon standard substrates. Reflectance and transmittance at normal incidence were also measured with a Varian Cary 6000i spectrometer in the spectral range of 200–1800 nm. As a result, the complex refractive index for all materials was evaluated by the WVASE32® software (J. A. Woollam Co, Version 3.774, Lincoln, NE, USA) while adopting oscillator models that that guaranteed a Kramers–Kronig consistency [41,43].

Normal incidence reflectance and angle resolved transmittance measurements were collected with an optical-fiber setup coupled with a charged coupled device spectrometer (Avantes AvaSpec-2048, 200−1150 nm, resolution 1.4 nm) (Avantes, Apeldoorn, Netherlands) and a deuterium−halogen Micropak DH2000BAL as a white light source, as previously described [44]. The optical response of the multilayered structure was modelled by using a Matlab® home-made software based on the transfer matrix method (TMM) formalism that was reported in [2]. For the calculation, we used the sample architecture (order and number of layers), the refractive index reported in Figure 1 for the IVP polymer, and the optical functions previously reported in literature for PVK and PAA as inputs [41]. The geometrical thicknesses of the single layers were instead retrieved as fitting parameter.
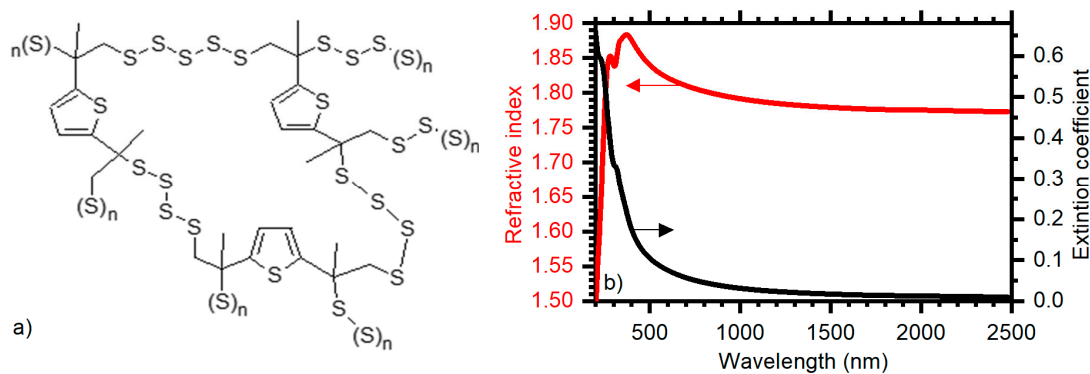
Figure 1. Structure (**a**) of the sulfur S-*r*-DIT copolymers that were obtained by the inverse vulcanization and complex refractive index spectrum (**b**) of the S-*r*-DIT copolymer with 70 wt% concentration; n (red line and scale) k (black line and scale).

3. Results and Discussion

The choice of the DIT comonomer, namely 2,5-diisopropenylthiophene, to be employed in the subsequent polymerization via the IV process originated from various considerations: (i) The heteroaromatic thiophene ring further enhances the refractive index of the resulting IVP by both its high electron density and the presence of the sulfur atom; (ii) the methyl groups borne by the isopropenyl substituents favor the reactivity in the IV radical process, with respect to the more commonly used vinyl functionalities; (iii) and, last but not least, the DIT molecule has never been synthesized before this work, even though it can be easily obtained by a cross-coupling reaction (CCR) starting from the commercially available 2,5-dibromothiophene substrate and a proper reactant that bears the isopropenyl moiety.

Among a number of cross-coupling reactions based on palladium catalysis, the one that has aroused particular interest both in academia and the industry for its experimental peculiarities (mild reaction conditions, the availability of a variety of precursors, functional-group compatibility, stability towards air and moisture, and the use of nontoxic and easily produced boronic acids), that ensure versatility and important applications is the condensation reaction of Suzuki-Miyaura [45–48]. Often referred to simply as Suzuki coupling, this reaction uses a boron derivative [R-BZ$_2$ (Z = R, OR)] as the carbon nucleophile partner for the formation of a new controlled C–C single bond [46]. The introduction of this class of reactants gave the classic catalytic cycle of palladium elements a novelty that had not yet been found in the common coupling reactions that make use of other metal-derivatives, so much so that it merited the awarding of the Nobel Prize in 2010 [49]. In this work, DIT was, for the first time, synthesized while adapting a Suzuki coupling protocol that is used for synthesizing 1,3,5-triisopropenylbenzene [32], as described in the Materials and Methods Section. Moreover, also for the first time, DIT was used as the comonomer in the inverse vulcanization with elemental sulfur.

As for the IV process, a specific method was developed to operate (i) in controlled conditions of temperature and atmosphere and (ii) to avoid DIT comonomer losses while efficiently stirring the reaction mixture. A series of IVPs, namely S-*r*-DIT copolymers at increasing sulfur contents (60, 70 and 80 wt%) were prepared. TGA measurements on the synthesized S-*r*-DIT copolymers demonstrated a good accordance between the residual mass (wt%) that was measured at 700 °C, essentially due to the carbonaceous residue that was derived from the DIT comonomer, and the amount of the latter in the reaction feed. Thermograms also revealed a relatively high thermal stability (well above 200 °C) of the copolymers. Both the temperatures of the degradation onset (starting from about 220 °C) and the maximum rate of mass loss (centered around 260 °C) were increased by increasing the sulfur percentage (respectively, of about 10 and 15 °C when passing from 60 to 80 wt% sulfur).

Figure 1a reports the schematic structure of the synthesized S-*r*-DIT copolymers. Figure 1b shows the real (n) and imaginary (k) part of the complex refractive index (n + ik) of the polymer with the intermediate 70 wt% sulfur concentration (n, red line; k, black line). The extinction coefficient was

almost structureless, and only two weak features at 230 and 300 nm could be detected and assigned to the sulfur chains, with an absorption tail extending to the near infrared [50]. The real part of the refractive index showed a relevant value out of resonance (1.77 at 2500 nm) and a normal dispersion up to the broad peak at 372 nm (n = 1.88). An additional structure was observed at 281 nm. These two peaks were the counterparts of the two resonances that were observed in the k spectrum. In the visible spectral range where the absorption tail was negligible, we could exploit the high refractive index (n = 1.83 at 600 nm) to grow one-dimensional photonic crystals with a high dielectric contrast. The availability of the spectrum of n + ik over a wide spectral range also allowed for the fine engineering and modelling of the optical response of the multilayers.

The DSC analysis of the copolymers revealed a quite low glass transition temperature, with values ranging from about 0 to −30 °C when passing from 60 to 80 wt% sulfur. Indeed, by increasing the percentage of the DIT comonomer, the points of reticulation increased, reducing segmental chain mobility. Still, the glass transition temperature of the IVPs remained very low and did not allow for the fabrication of multilayers with good optical quality. Indeed, the low IVP viscosity led to the washout of the polymers during subsequent depositions. For this reason, to increase the IVPs' processability, we blended them with commercial PVK, which represented the transparent polymer with the higher refractive index and better processability that is available on the market [41]. The new blends were then spun-cast alternatively to PAA as a low refractive index medium to fabricate three DBR structures (Figure 2a). Figure 2 displays the reflectance spectra—different line colors correspond to different points on the sample surface—and the digital photographs of the surfaces of these DBRs. When the lower amount of sulfur was employed (sulfur to monomer ratio 60:40), the sample surface presented a greyish color that arose from the optical response reported in Figure 2b. The spectrum showed a weak and broad reflectance structure at about 420 nm that did not have enough intensity to provide surface coloration but could be assigned to the photonic band gap (PBG) of a very disordered structure. In spite of that, the spectra backgrounds that were collected in different spots of the surface presented a quite homogeneous interference pattern, showing that the upper and lower DBR interfaces possessed good optical quality and plane parallel surfaces [2]. These apparently opposite results suggested a reduced control and reproducibility of the thickness and interfacial roughness for the inner layers only, indicating that the multilayer behaved more similarly to a composite effective medium than to a photonic crystal. These results indicated that the polymer containing the 60 wt% of sulfur was not able to be processed to obtain photonic structures by spin-coating deposition. Upon increasing the amount of sulfur to 70 wt% with respect to the DIT organic component (S:M ratio = 70:30) we noticed the sample became violet and highly homogenous, as demonstrated in Figure 2c. In this case, the spectra were characterized by a sharp and intense reflectance peak (R = 80%) that was assigned to the PBG at 430 nm. The superimposition of the collected spectra further supported the homogeneity of the photonic crystal structure, including the internal layers. In this case, the interference fringe's visibility was higher than in the previously described sample, demonstrating a better quality of the overall structure due to the improved processability of the IVP–PVK blend. Upon a further increase of the amount of sulfur to 80 wt%, the quality of the ensuing structure decreased again, and only an interference pattern was detectable in the spectra (Figure 2d). In this case, the homogeneity was also lacking, and no evident structural coloration could be detected on the sample surface, which appeared greyish. These data confirm that only the S-*r*-DIT copolymer with 70 wt% in sulfur allowed for films with an optical quality that was sufficient for the fabrication of DBR structures.
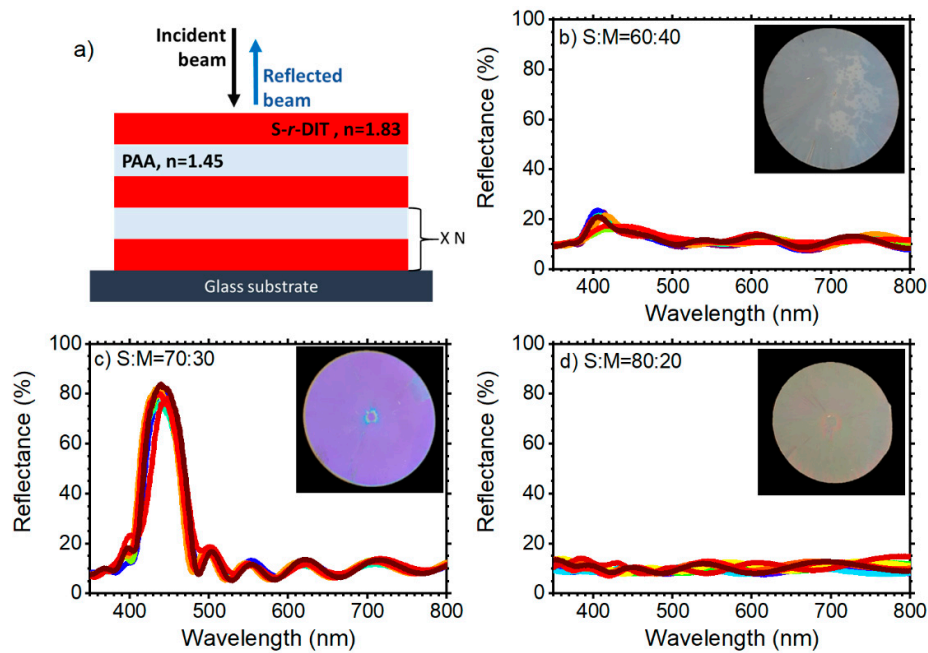
Figure 2. (**a**) Schematic and (**b**–**d**) reflectance spectra and surface photographs of three inverse vulcanized polymer: poly(*N*-vinyl carbazole)–polyacrylic acid (IVP:PVK–PAA) distributed Bragg reflectors (DBRs) made of 10.5 bilayers where the IVPs were synthesized from reactant mixtures that contained 60 wt% (**b**), 70 wt% (**c**) and 80 wt% (**d**) of sulfur with respect to 2,5-diisopropenilthiophene.

To further characterize the optical quality of the DBR structure, Figure 3 reports the calculated normal incidence reflectance spectra for the sample prepared with the IVP that contained 70 wt% of sulfur (compare with Figure 2c), together with both the theoretical and experimental angular dispersion of the PBG. In detail, Figure 3a shows that the experimental and modelled reflectance spectra of the sample were in full agreement. As described in the Materials and Methods section, the reflectance data were modelled by using the refractive index of the polymer components and the sample geometry as inputs, while the layer thicknesses were the fitting parameters. The latter resulted in 43 nm for the IVP polymer and 95 nm for PAA. These data also agreed with the polymer concentration that was used during the layer deposition (see Materials and Methods section). As widely reported in the literature for Bragg reflectors [2,13,41,51–55], these modelling data, together with the high homogeneity of the sample spectra reported in Figure 2c, confirm the presence highly homogeneous layers with controlled thickness. [2,13,41,51–55] To further confirm the PBG assignment, we also recorded its angular dispersion and compared it with theory. Figure 3b schematizes the measurement set-up. The sample was placed in the path of a collimated light beam and tilted to collect the transmittance spectrum at different light incidence angles. In the plot of Figure 3b, this angle is reported on the y-axis, and light wavelength is reported in the x-axis. The color scale, indicated in the sidebar, represents the transmittance intensity such that the blue shades show the lower intensities and the red shades the higher ones. The data are reported for unpolarized light only, as in agreement with theory [2] and previous reports [41], the Brewster angle cannot be detected due to the IVP polymer and glass absorbance which predominates the PBG spectral feature at wavelength shorter than 370 nm. The PBG, which is indeed visible in blue tones in the plot, was initially detected at 430 nm at normal incidence, as expected from Figure 2b. The low intensity signal detected slightly above 350 nm was instead assigned to the absorbance of the glass substrate and of the S-*r*-DIT copolymer itself. By increasing the angle of incidence of light, the spectral position of the PBG structure shifted to the short wavelength side of the spectrum, as expected from the theory [2,55]. Indeed, the spectral peak position of the PBG (black squares) is compared with theoretical predictions (red dots) in Figure 3d, where theoretical and experimental data are again in full agreement. These data unambiguously confirm the formation of

a PBG in the DBR structures that were grown with the IVP. The good optical quality of the structure and its reproducibility are very promising for further development in the fields of photonics and sensing [2].
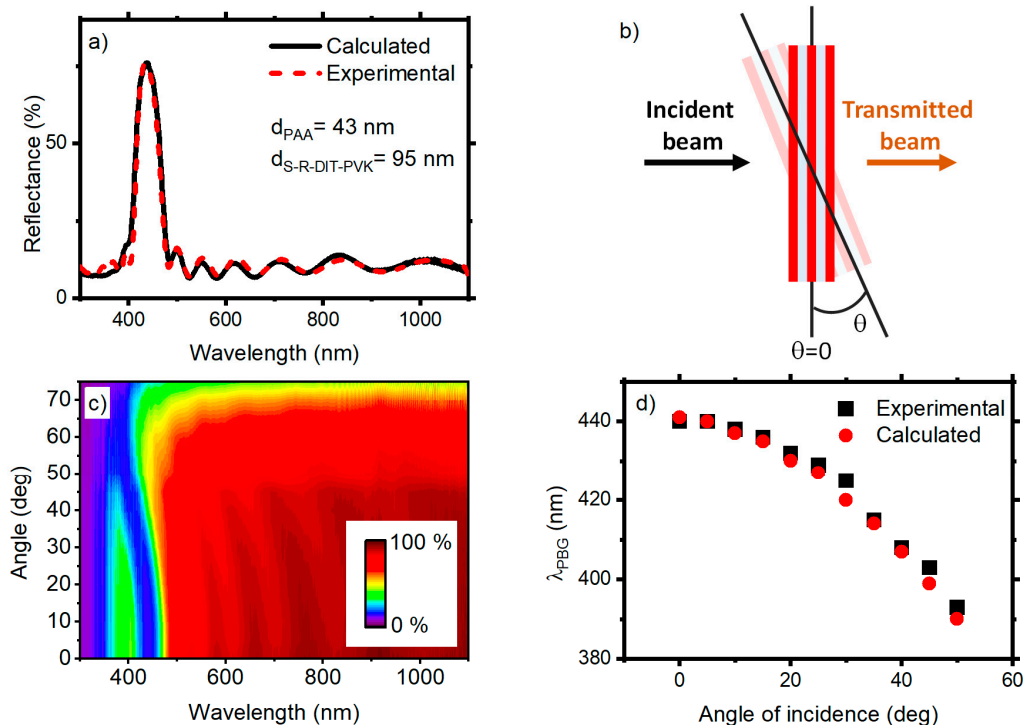

Figure 3. (**a**) Comparison between experimental and modelled normal incidence reflectance of the DBR that was made by using IVP with an initial sulfur concentration of 70 wt%; (**b**) schematic of the transmittance measurement set-up; (**c**) contour plot of the angular resolved transmittance spectra that were collected for a 10.5 bilayer DBRs; and (**d**) comparison between the experimental and theoretical spectral positions of the PBG.

Interestingly, notwithstanding the absorbance of the IVP in the ultraviolet and visible spectral range (Figure 2), the blend with PVK allowed us to tune the PBG within this spectral range without incurring in strong light absorption phenomena. This allowed us to employ the IVP in a very broad spectral range spanning from 400 to 2600 nm, thus making this material promising not only for the telecommunication windows but also for light control applications including lasing [2,13]. These data confirm that despite the low T_g of the IVP, it is possible to obtain polymer DBRs with good optical quality and with relatively high dielectric contrast by employing simple polymer blends. These systems are promising for the development of highly confined, all-polymer photonic structures that are processable from solution or even by melt processing on a large area.

4. Conclusions

In summary, we developed new, inversely vulcanized polymers that are endowed with a very high refractive index (n = 1.83 at 600 nm) and were obtained through the simple copolymerization of molten elemental sulfur with 2,5-diisopropeniltiofene comonomer in different ratios. The new IVPs were blended with PVK to enhance processability, thus allowing for the obtainment of very high optical quality all-polymer planar photonic crystals. The possibility to blend the IVPs with a commercial polymer led to highly processable high refractive index media that were characterized by optical transparency in the spectral range from the near ultraviolet to near infrared. Furthermore, the large availability of sulfur wastes makes these new systems highly promising and technologically relevant for a variety of applications spanning from lighting devices to light emission control and lasing.

References

1. Laussy, F.P. *Microcavities*; Oxford University Press: New York, NY, USA, 2017.
2. Lova, P.; Manfredi, G.; Comoretto, D. Advances in functional solution processed planar one-dimensional photonic crystals. *Adv. Opt. Mater.* **2018**, *6*, 1800726–1800730. [CrossRef]
3. Berti, L.; Cucini, M.; Di Stasio, F.; Comoretto, D.; Galli, M.; Marabelli, F.; Manfredi, N.; Marinzi, C.; Abbotto, A. Spectroscopic investigation of artificial opals infiltrated with a heteroaromatic quadrupolar dye. *J. Phys. Chem. C* **2010**, *114*, 2403–2413. [CrossRef]
4. Dodero, A.; Vicini, S.; Alloisio, M.; Castellano, M. Sodium alginate solutions: Correlation between rheological properties and spinnability. *J. Mater. Sci.* **2019**, *54*, 8034–8046. [CrossRef]
5. Vicini, S.; Mauri, M.; Vita, S.; Castellano, M. Alginate and alginate/hyaluronic acid membranes generated by electrospinning in wet conditions: Relationship between solution viscosity and spinnability. *J. Appl. Polym. Sci.* **2018**, *135*, 46390. [CrossRef]
6. Zhou, J.; Singer, K.D.; Lott, J.; Song, H.; Wu, Y.; Andrews, J.; Baer, E.; Hiltner, A.; Weder, C. All-polymer distributed feedback and distributed Bragg-reflector lasers produced by roll-to-roll layer-multiplying co-extrusion. *Nonlinear Opt. Quantum Opt.* **2010**, *41*, 59–71.
7. Ko, Y.-L.; Tsai, H.-P.; Lin, K.-Y.; Chen, Y.-C.; Yang, H. Reusable macroporous photonic crystal-based ethanol vapor detectors by doctor blade coating. *J. Colloid Interface Sci.* **2017**, *487*, 360–369. [CrossRef]
8. Song, H.; Singer, K.; Lott, J.; Wu, Y.; Zhou, J.; Andrews, J.; Baer, E.; Hiltner, A.; Weder, C. Continuous melt processing of all-polymer distributed feedback lasers. *J. Mater. Chem.* **2009**, *19*, 7520–7524. [CrossRef]
9. TORAY. Available online: http://www.toray.com/ (accessed on 27 January 2020).
10. 3M DICHROIC. Available online: https://www.3m.com/3M/en_US/company-us/all-3m-products/~{}/3M-Dichroic-Films-for-Architectural-Laminated-Glass/?N=5002385+3291680356&rt=rud (accessed on 27 January 2020).
11. Iasilli, G.; Francischello, R.; Lova, P.; Silvano, S.; Surace, A.; Pesce, G.; Alloisio, M.; Patrini, M.; Shimizu, M.; Comoretto, D.; et al. Luminescent solar concentrators: Boosted optical efficiency by polymer dielectric mirrors. *Mater. Chem. Front.* **2019**, *3*, 429–436. [CrossRef]
12. Lova, P.; Giusto, P.; Stasio, F.D.; Manfredi, G.; Paternò, G.M.; Cortecchia, D.; Soci, C.; Comoretto, D. All-polymer methylammonium lead iodide perovskite microcavity. *Nanoscale* **2019**, *11*, 8978–8983. [CrossRef]
13. Manfredi, G.; Lova, P.; Di Stasio, F.; Rastogi, P.; Krahne, R.; Comoretto, D. Lasing from dot-in-rod nanocrystals in planar polymer microcavities. *RSC Adv.* **2018**, *8*, 13026–13033. [CrossRef]
14. Robbiano, V.; Paternò, G.M.; La Mattina, A.A.; Motti, S.G.; Lanzani, G.; Scotognella, F.; Barillaro, G. Room-temperature low-threshold lasing from monolithically integrated nanostructured porous silicon hybrid microcavities. *ACS Nano* **2018**, *12*, 4536–4544. [CrossRef]
15. Liu, J.-G.; Ueda, M. High refractive index polymers: Fundamental research and practical applications. *J. Mater. Chem.* **2009**, *19*, 8907–8919. [CrossRef]
16. Higashihara, T.; Ueda, M. Recent progress in high refractive index polymers. *Macromolecules* **2015**, *48*, 1915–1929. [CrossRef]
17. Radice, S.V.; Gavezotti, P.; Simeone, G.; Albano, M.; Canazza, G.; Congiu, S. Photonic Crystals. WO PCT/EP2014/055590, 20 March 2014.
18. Radice, S.V.; Srinivasan, P.; Comoretto, D.; Gazzo, S. One-Dimensional Planar Photonic Crystals Including Fluoropolymer Compositions and Corresponding Fabrication Methods. WO 2016/087439 A1, 9 June 2016.
19. Russo, M.; Campoy-Quiles, M.; Lacharmoise, P.; Ferenczi, T.A.M.; Garriga, M.; Caseri, W.R.; Stingelin, N. One-pot synthesis of polymer/inorganic hybrids: Toward readily accessible, low-loss, and highly tunable refractive index materials and patterns. *J. Polym. Sci. Part B Polym. Phys.* **2012**, *50*, 65–74. [CrossRef]

20. Giusto, P.; Lova, P.; Manfredi, G.; Gazzo, S.; Srinivasan, B.; Radice, S.V.; Comoretto, D. Colorimetric detection of perfluorinated compounds by all-polymer photonic transducers. *ACS Omega* **2018**, *3*, 7517–7522. [CrossRef]

21. Flaim, T.D.; Wang, Y.; Mercado, R. High-refractive-index polymer coatings for optoelectronics applications. In Proceedings of the Optical Systems Design, St. Etienne, France, 25 February 2004; p. 12.

22. Shimizu, W.; Nakamura, S.; Sato, T.; Murakami, Y. Creation of high-refractive-index amorphous titanium oxide thin films from low-fractal-dimension polymeric precursors synthesized by a sol–gel technique with a hydrazine monohydrochloride catalyst. *Langmuir* **2012**, *28*, 12245–12255. [CrossRef]

23. Lu, C.; Yang, B. High refractive index organic-inorganic nanocomposites: Design, synthesis and application. *J. Mater. Chem.* **2009**, *19*, 2884–2901. [CrossRef]

24. Comoretto, D.; Dellepiane, G.; Cuniberti, C.; Rossi, L.; Borghesi, A.; LeMoigne, J. Photoinduced absorption of oriented poly 1,6-di(*N*-carbazolyl)-2,4-hexadiyne. *Phys. Rev. B* **1996**, *53*, 15653–15659. [CrossRef]

25. Comoretto, D.; Cuniberti, C.; Musso, G.F.; Dellepiane, G.; Speroni, F.; Botta, C.; Luzzati, S. Optical properties and long-lived charged photoexcitations in polydiacetylenes. *Phys. Rev. B* **1994**, *49*, 8059–8066. [CrossRef]

26. Ravnik, M.; Alexander, G.P.; Yeomans, J.M.; Žumer, S. Three-dimensional colloidal crystals in liquid crystalline blue phases. *Proc. Natl. Acad. Sci. USA* **2011**, *108*, 5188–5192. [CrossRef]

27. Nussbaumer, R.J.; Caseri, W.R.; Smith, P.; Tervoort, T. Polymer-TiO$_2$ nanocomposites: A route towards visually transparent broadband uv filters and high refractive index materials. *Macromol. Chem. Phys.* **2003**, *288*, 44–49. [CrossRef]

28. Ogata, T.; Yagi, R.; Nakamura, N.; Kuwahara, Y.; Kurihara, S. Modulation of polymer refractive indices with diamond nanoparticles for metal-free multilayer film mirrors. *ACS Appl. Mater. Interfaces* **2012**, *4*, 3769–3772. [CrossRef] [PubMed]

29. Gher, R.J.; Boyd, R.W. Optical properties of nanostructured optical materials. *Chem. Mater.* **1996**, *8*, 1807–1819. [CrossRef]

30. Gaëtan, W.; Rolando, F.; Stefan, S.; Libero, Z. Nanoporous films with low refractive index for large-surface broad-band anti-reflection coatings. *Macromol. Chem. Phys.* **2010**, *295*, 628–636.

31. Gazzo, S.; Manfredi, G.; Pötzsch, R.; Wei, Q.; Alloisio, M.; Voit, B.; Comoretto, D. High refractive index hyperbranched polyvinylsulfides for planar one-dimensional all-polymer photonic crystals. *J. Polym. Sci. Part B Polym. Phys.* **2016**, *54*, 73–80. [CrossRef]

32. Kleine, T.S.; Nguyen, N.A.; Anderson, L.E.; Namnabat, S.; LaVilla, E.A.; Showghi, S.A.; Dirlam, P.T.; Arrington, C.B.; Manchester, M.S.; Schwiegerling, J.; et al. High refractive index copolymers with improved thermomechanical properties via the inverse vulcanization of sulfur and 1,3,5-triisopropenylbenzene. *ACS Macro Lett.* **2016**, *5*, 1152–1156. [CrossRef]

33. Anderson, L.E.; Kleine, T.S.; Zhang, Y.; Phan, D.D.; Namnabat, S.; LaVilla, E.A.; Konopka, K.M.; Ruiz Diaz, L.; Manchester, M.S.; Schwiegerling, J.; et al. Chalcogenide hybrid inorganic/organic polymers: Ultrahigh refractive index polymers for infrared imaging. *ACS Macro Lett.* **2017**, *6*, 500–504. [CrossRef]

34. Chung, W.J.; Griebel, J.J.; Kim, E.T.; Yoon, H.; Simmonds, A.G.; Ji, H.J.; Dirlam, P.T.; Glass, R.S.; Wie, J.J.; Nguyen, N.A.; et al. The use of elemental sulfur as an alternative feedstock for polymeric materials. *Nat. Chem.* **2013**, *5*, 518–524. [CrossRef]

35. Griebel, J.J.; Glass, R.S.; Char, K.; Pyun, J. Polymerizations with elemental sulfur: A novel route to high sulfur content polymers for sustainability, energy and defense. *Prog. Polym. Sci.* **2016**, *58*, 90–125. [CrossRef]

36. Griebel, J.J.; Nguyen, N.A.; Namnabat, S.; Anderson, L.E.; Glass, R.S.; Norwood, R.A.; Mackay, M.E.; Char, K.; Pyun, J. Dynamic covalent polymers via inverse vulcanization of elemental sulfur for healable infrared optical materials. *ACS Macro Lett.* **2015**, *4*, 862–866. [CrossRef]

37. Ramarad, S.; Khalid, M.; Ratnam, C.T.; Chuah, A.L.; Rashmi, W. Waste tire rubber in polymer blends: A review on the evolution, properties and future. *Prog. Mater. Sci.* **2015**, *72*, 100–140. [CrossRef]

38. Griebel, J.J.; Namnabat, S.; Kim, E.T.; Himmelhube, R.; Moronta, D.H.; Chung, W.J.; Simmonds Adam, G.; Kim Kyung, J.; Van der Laan, J.; Nguyen Ngoc, A.; et al. New infrared transmitting material via inverse vulcanization of elemental sulfur to prepare high refractive index polymers. *Adv. Mater.* **2014**, *26*, 3014–3018. [CrossRef] [PubMed]

39. Concidian, D. Sulfur (in biological systems). In *Van Nostrand's Scientific Encyclopedia*; D. Van Nostrand Company, Inc.: Hoboken, NJ, USA, 2005. [CrossRef]

40. Boyd, D.A. Sulfur and its role in modern materials science. *Angew. Chem. Int. Ed.* **2016**, *55*, 15486–15502. [CrossRef] [PubMed]

41. Lova, P.; Grande, V.; Manfredi, G.; Patrin, M.; Herbst, S.; Würthner, F.; Comoretto, D. All-polymer photonic microcavities doped with perylene bisimide J-aggregates. *Adv. Opt. Mater.* **2017**, *5*, 1700523. [CrossRef]

42. Manfredi, G.; Lova, P.; Di Stasio, F.; Krahne, R.; Comoretto, D. Directional fluorescence shaping and lasing in all-polymer microcavities doped with CdSe/CdS dot-in-rod nanocrystals. In Proceedings of the 2017 European Conference on Lasers and Electro-Optics and European Quantum Electronics Conference, Munich, Germany, 25–29 June 2017.

43. J.A. Woollam Co. *WVASE32® Software*; J.A. Woollam Co.: Lincoln, NE, USA, 2006.

44. Lova, P.; Cortecchia, D.; Soci, C.; Comoretto, D. Solution processed polymer-ABX$_4$ perovskite-like microcavities. *Appl. Sci.* **2019**, *9*, 5203. [CrossRef]

45. Miyaura, N.; Suzuki, A. Stereoselective synthesis of arylated (E)-alkenes by the reaction of alk-1-enylboranes with aryl halides in the presence of palladium catalyst. *J. Chem. Soc. Chem. Commun.* **1979**. [CrossRef]

46. Miyaura, N.; Suzuki, A. Palladium-catalyzed cross-coupling reactions of organoboron compounds. *Chem. Rev.* **1995**, *95*, 2457–2483. [CrossRef]

47. American Chemical Society. Green chemical syntheses and processes. In *Green Chemical Syntheses and Processes*; American Chemical Society: Washington, DC, USA, 2000; Volume 767, pp. 1–5.

48. Hooshmand, S.E.; Heidari, B.; Sedghi, R.; Varma, R.S. Recent advances in the Suzuki–Miyaura cross-coupling reaction using efficient catalysts in eco-friendly media. *Green Chem.* **2019**, *21*, 381–405. [CrossRef]

49. Nobel Prize in Chemistry 2010. Available online: https://www.nobelprize.org/prizes/chemistry/2010/summary/ (accessed on 27 January 2020).

50. Chen, J.; Liu, L.; Weng, L.; Lin, Y.; Liao, L.; Wang, C.; Yang, J.; Wu, Z. Synthesis and properties evolution of a family of tiara-like phenylethanethiolated palladium nanoclusters. *Sci. Rep.* **2015**, *5*, 16628. [CrossRef]

51. Lova, P.; Cortecchia, D.S.; Krishnamoorthy, H.N.; Giusto, P.; Bastianini, C.; Bruno, A.; Comoretto, D.; Soci, C. Engineering the emission of broadband 2D perovskites by polymer distributed Bragg reflectors. *ACS Photonics* **2018**, *5*, 867–874. [CrossRef]

52. Manfredi, G.; Lova, P.; Di Stasio, F.; Krahne, R.; Comoretto, D. Directional fluorescence spectral narrowing in all-polymer microcavities doped with CdSe/CdS dot-in-rod nanocrystals. *ACS Photonics* **2017**, *4*, 1761–1769. [CrossRef]

53. Joannopulos, J.D.; Meade, R.D.; Win, J.N. *Photonic Crystals: Molding the Flow of the Light*; Princeton University Press: Princeton, NJ, USA, 1995.

54. Unger, K.; Resel, R.; Czibula, C.; Ganser, C.; Teichert, C.; Jakopic, G.; Canazza, G.; Gazzo, S.; Comoretto, D. Distributed Bragg reflectors: Morphology of cellulose acetate and polystyrene multilayers. In Proceedings of the 2014 16th International Conference on Transparent Optical Networks (ICTON), Graz, Austria, 6–10 July 2014; pp. 1–4.

55. Comoretto, D. *Organic and Hybrid Photonic Crystals*; Springer: Cham, Switzerland, 2015.